

Space-time sensors using multiple-wave atomic levitation.

F. Impens^{1,2} and Ch. J. Bordé^{1,3}

¹ SYRTE, Observatoire de Paris, 77 Avenue Denfert-Rochereau, 75014 Paris, France

² Instituto de Física, Universidade Federal do Rio de Janeiro. Caixa Postal 68528, 21941-972 Rio de Janeiro, RJ, Brasil and

³ Laboratoire de Physique des Lasers, Institut Galilée, F-93430 Villetaneuse, France

Optical atomic clocks are promising tools to investigate basic physics through fundamental tests [1, 2]. The best clocks to date [3, 4, 5] control the atomic motion by trapping the sample in an optical lattice [6] and then interrogate the atomic transition by shining on these atoms a distinct laser of controlled frequency. In order to perform both operations simultaneously and with the same laser field, we propose to use instead the levitation of a Bose-Einstein condensate through multiple-wave atomic interferences [7, 8, 9]. The levitating condensate experiences a coherent localization in momentum and a controlled diffusion in altitude. The sample levitation is bound to a set of resonance conditions [10, 11] used either for frequency or for acceleration measurements. The chosen vertical geometry solves the limitations imposed by the sample free fall in previous optical clocks [12] using also atomic interferences. This configuration allows for multiple-wave interference effects, which maintain the atomic population in levitation and yield a sensitivity improvement. This setup constitutes an attractive alternative to current atomic clocks and gravimeters [11, 13].

The light-matter interaction enables the exchange of momentum between an electromagnetic field and a collection of atoms: each atom emitting or absorbing a photon experiences simultaneously a change of internal level and a recoil reflecting the global momentum conservation. This well-controlled momentum transfer can be used to engineer correlations between the motional and the internal atomic state. This is the principle underlying Bordé-Ramsey atom interferometers [14, 15, 16], building blocks of our system. Such interferometers consist in the illumination of travelling two-level atoms with a first pair of light pulses separated temporally and propagating in the same direction [Fig.1], followed by a second pair of pulses coming from the opposite direction. Each pulse operates a $\pi/2$ -rotation on the vector representing the atomic density matrix on the Bloch sphere [17]: applied on a given internal state, it creates a quantum superposition of two atomic states with distinct internal levels and momenta. Horizontal Bordé-Ramsey interferometers have been used to build optical clocks [12]. This system presents, however, two drawbacks: the free fall of the atoms through the transverse lasers probing their transition limits the interrogation time and induces undesirable frequency shifts [18]. This led the metrology community to privilege experiments built around atomic

traps [6], able to control the sample position. This Letter proposes instead to circumvent these limitations with a multiple-wave atom interferometer [7, 8, 9] in levitation, which comprises a succession of vertical Bordé-Ramsey atom interferometers. This strategy combines the best aspects of optical clocks based on atom traps and on atom interferometers: it prevents the sample free fall without using optical potentials likely to cause spurious frequency shifts. The recent experimental achievement [11] of a sustainable levitation of coherent atomic waves with synchronized light pulses [10] strongly supports the feasibility of this method.

Our purpose is to provide a controlled vertical momentum transfer to the atoms, eventually enabling their levitation, through the repetition of a four vertical $\pi/2$ -pulse sequence. Momentum kicks are achieved by performing two successive population transfers with vertical pulses propagating in opposite directions: starting from the adequate atomic state, one obtains successively the absorption of an upward photon followed by the emission of a downward one, imparting a net upward momentum to the atoms. This leads us to consider the point illustrated in Fig. 1: when do two time-separated $\pi/2$ -pulses realize a full population transfer? To achieve

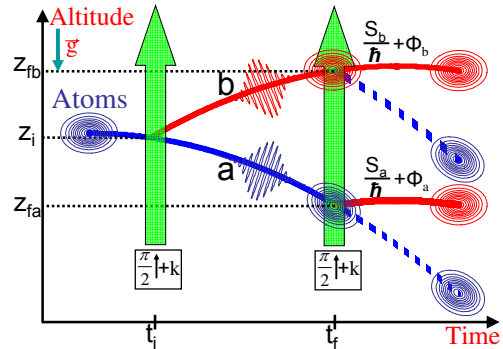


FIG. 1: Action of a pair of copropagating $\pi/2$ -pulses on a free-falling atomic wave-packet. The phase difference between the two outgoing wave-packets comes from the classical action and laser phase acquired on each path, and from the distance of their centers.

this, one must indeed compensate the phase induced by the external atomic motion in the time-interval through fine-tuned laser phases. This phase adjustment is at the heart of our proposal, since it provides the resonance condition serving for the laser frequency stabilization in the clock operation. The $\pi/2$ -pulse sequence then yields

a *conditional* momentum transfer, controlled by this resonance condition, which distinguishes this process from atomic Bloch oscillations [19, 20]. Long π -pulses, realizing conditional population transfers [16], could also perform such levitation [10, 11]. Yet there are several benefits in privileging $\pi/2$ -pulses: the atomic illumination time is drastically reduced, the pulses address a broader distribution of atomic momenta, and a better sensitivity is obtained through a wider interferometric area [16]. To obtain the resonance condition, we consider a dilute sample of two-level atoms evolving in the gravity field -taken as uniform- according to the Hamiltonian $H = \frac{p^2}{2m} + mgz$. It is initially in the lower state a and described by the Gaussian wave-function $\psi_a(\mathbf{r}, t_0) =$

$$\frac{\pi^{-3/2}}{\sqrt{w_{x0}w_{y0}w_{z0}}} e^{-\frac{1}{2} \left(\frac{(x-x_i)^2}{w_{x0}^2} + \frac{(y-y_i)^2}{w_{y0}^2} + \frac{(z-z_i)^2}{w_{z0}^2} \right) + \frac{i}{\hbar} \mathbf{p}_{ia}(t_0) \cdot (\mathbf{r} - \mathbf{r}_i)}$$

After two $\pi/2$ -pulses, performed at the times t_i and $t_f = t_i + T$, the initial wave-packet has been split into four packets following two possible intermediate trajectories. The excited wave-function receives two wave-packet contributions coming from either path and associated with the absorption of a photon at times t_i and t_f , of common central momentum $\mathbf{p}_f = \mathbf{p}_i + \hbar\mathbf{k} + mgT$ and respective central positions \mathbf{r}_{fa} and \mathbf{r}_{fb} . These wave-packets acquire a phase $S_{a,b}/\hbar$ reflecting the action on each path [21] and a laser phase $\phi_{a,b}$ evaluated at their center for the corresponding interaction time. Both contributions to the excited state are phase-matched if the following relation is verified

$$-\mathbf{p}_f \cdot \mathbf{r}_{f,a} + S_a + \hbar\phi_a = -\mathbf{p}_f \cdot \mathbf{r}_{f,b} + S_b + \hbar\phi_b. \quad (1)$$

The terms $\mathbf{p}_f \cdot \mathbf{r}_{f,a,b}$ reflect the atom-optical path difference between both wave-packets at their respective centers. The central time $t_c = (t_i + t_f)/2$ is used as phase reference for the two successive pulses. The phases ϕ_b and ϕ_a , provided respectively by the first and the second $\pi/2$ -pulse, read $\phi_{b,a} = \mathbf{k} \cdot \mathbf{r}_{i,fa} - \omega_{1,2}(t_{i,f} - t_c) + \phi_{1,2}^0$. Condition (1) is fulfilled if the frequencies $\omega_{1,2}$ of the first and second pulses are set to their resonant values

$$\omega_{1,2} = \frac{1}{\hbar} \left(E_b + \frac{(\mathbf{p}_{1,2} + \hbar\mathbf{k})^2}{2m} - E_a - \frac{p_{1,2}^2}{2m} \right) \quad (2)$$

with $\mathbf{p}_1 = \mathbf{p}_i$ and $\mathbf{p}_2 = \mathbf{p}_i + mgT$, and if the constant phases $\phi_{1,2}^0$ satisfy $\phi_1^0 = \phi_2^0$. If these conditions are fulfilled, and if the sample coherence length w is much larger than the final wave-packet separation $|\mathbf{r}_{f,a} - \mathbf{r}_{f,b}|$, one obtains an almost fully constructive interference in the excited state. The succession of two $\pi/2$ -pulses then mimics very efficiently a single π -pulse, the quantum channel to the lower state being shut off by destructive interferences. A key point is that condition (1), expressing the equality of the quantity $I = -\mathbf{p}_f \cdot \mathbf{r}_f + S + \hbar\phi$ for both paths, is independent of the initial wave-packet position. This property allows one to address simultaneously the numerous wave-packets generated in the $\pi/2$ pulse sequence.

Applying a second sequence of two $\pi/2$ pulses with downward wave-vectors, one obtains a vertical Bordé-

interferometer bent by the gravity field sketched in Fig. 2. Starting with a sufficiently coherent sample in

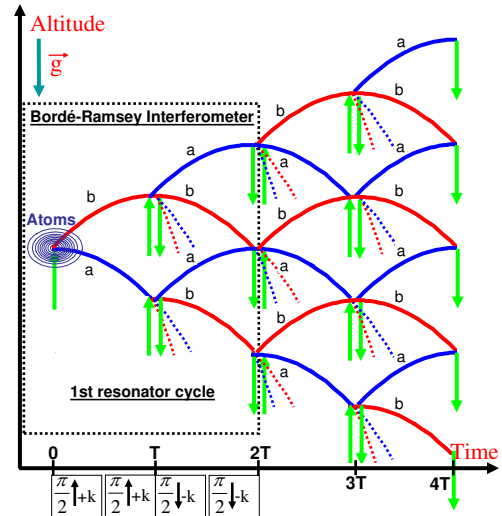


FIG. 2: Levitating atomic trajectories in the sequence of pulses spanning the interferometric area. The first four pulses generate a vertical Bordé-Ramsey interferometer. The central positions of the wave-packets explore a network of paths which doubles at each laser pulse.

the lower state, and with well adjusted frequencies (2) and ramp slopes, the previous discussion shows that a net momentum transfer of $2\hbar\mathbf{k}$ is provided to each atom during the interferometric sequence. For the special interpulse duration

$$T := T^0 = \frac{\hbar k}{mg}, \quad (3)$$

these atoms end up in the lower state with their initial momentum. Two major benefits are then expected. First, the periodicity of the sample motion in momentum gives rise to levitation. Second, only two frequencies, given by (2), are involved in the successive resonant pairs of $\pi/2$ pulses. In particular, the first and the fourth pulse of the Bordé-Ramsey interferometer, as well as the second and the third one, correspond to identical resonant frequencies: $\omega_1^0 = \omega_4^0$ and $\omega_2^0 = \omega_3^0$.

If the previous conditions are fulfilled, the repetition of the interferometer sequence gives rise to a network of levitating paths - sketched in Fig. 2 - reflecting the diffusion of the atomic wave in the successive light pulses. The same laser field is used to levitate the sample and to perform its interrogation, generating a clock signal based on either one of the two frequencies ω_1^0, ω_2^0 . Our measurement indeed rests on the double condition (2, 3), which must be fulfilled to ensure this periodic motion: should the parameters $(T, \omega_{1,2,3,4})$ differ from their resonant values $(T^0, \omega_{1,2,3,4}^0)$, the outgoing channels would open again and induce losses in the levitating cloud, which can be tracked by a population measurement. We

expect multiple-wave interferences to induce a narrowing of the resonance curve associated with the levitating population around this condition.

We have investigated this conjecture through a numerical simulation. The considered free-falling sample is taken at zero temperature, sufficiently diluted to render interaction effects negligible, and described initially by a macroscopic Gaussian wave-function. Its propagation in-between the pulses is obtained by evaluating a few parameters: central position and momentum following classical dynamics, widths satisfying $w_{x,y,z}^2(t) = w_{x,y,z}^2 + \frac{\hbar^2}{4m^2 w_{x,y,z}^2} (t - t_0)^2$, and a global phase proportional to the action on the classical path [21]. The diffusion of atomic packets on the short light pulses is efficiently modeled by a position-dependent Rabi matrix [16] evaluated at the packet center. While the evolution of each wave-packet is very simple, their number -doubling at each light pulse- makes their book-keeping a computational challenge. This difficulty, intrinsic to the classical simulation of an entangled quantum state, has limited our investigation to a sequence of sixteen pulses, involving 28 levitating Bordé-Ramsey interferometers associated with the resonant paths. The number of atomic waves involved ($N \simeq 64000$) is nonetheless sufficient to probe multiple-wave interference effects.

The atomic transition used in this setup should have level lifetimes longer than the typical interferometer duration (ms). Possible candidates are the Sr, Yb and Hg atoms, which have a narrow clock transition in their internal structure. These atoms should be cooled at a temperature in the nano-Kelvin range, preferably in a vertical cigar-shaped condensate, in order to guarantee a sufficient overlap of the interfering wave-packets and preserve a significant levitating atomic population. We consider a cloud of coherence length $w = 100 \mu\text{m}$ much larger than the wave-packets separation $2h \simeq 15 \mu\text{m}$. Fig. 3 shows the levitating and the falling atomic population in the lower state as a function of the frequency shift $\delta\omega$ from the resonant frequencies $\omega_{1,2,3,4}^0$. It reveals a fully constructive interference in the levitating arches when resonance conditions are fulfilled, as well as the expected narrowing of the central fringe associated with the levitating wave-packets. Falling wave-packets yield secondary fringe patterns with shifted resonant frequencies, which induce an asymmetry in the central fringe if the total lower state population is monitored. This effect, critical for a clock operation, can nonetheless be efficiently attenuated by limiting the detection zone to the vicinity of the levitating arches. This strategy improves as the levitation time increases: the main contribution to the “falling” background comes then from atoms with a greater downward momentum and thus further away from the detection zone. Besides, multiple wave interferences sharpen the symmetric “levitating” central fringe fast enough to limit the effect of the asymmetric background of falling fringes. Considering a shift δT from the resonant duration T_0 , one obtains also a central fringe

narrowing as the number of pulses increases and thus an improved determination of acceleration g through condition (3) [10, 11]. Multiple wave interferences thus improve the setup sensitivity in both the inertial and frequency domains.

To keep the sample within the laser beam diameter, it is necessary to use a transverse confinement, which may be obtained by using laser waves of spherical wave-front for the pulses [10]. In contrast to former horizontal clocks [12], the atomic motion is here collinear to the light beam, which reduces the frequency shift resulting from the wave-front curvature. A weak-field treatment, to be published elsewhere, shows that this shift is proportional to the ratio $\Delta\omega_{curv.} \propto k\langle v_{\perp}^2 \rangle T/R$, involving the average square transverse velocity $\langle v_{\perp}^2 \rangle$ and the field radius of curvature R at the average altitude of the levitating cloud.

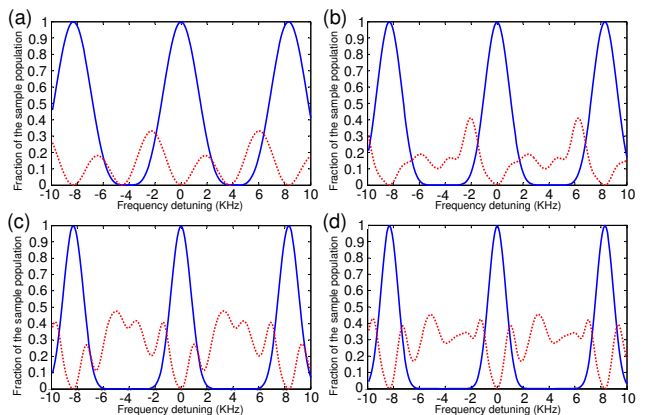


FIG. 3: Fraction of the total sample population levitating (full line) and falling (dashed line) in state a after one, two, three and four sequences of four pulses as a function of the frequency detuning $\delta\omega$ (kHz) ($\omega_{1,2,3,4} := \omega_{1,2,3,4}^0 + \delta\omega$) and for a resonant interferometer duration $2T^0 \simeq 1.5 \text{ ms}$, with pulses of Rabi pulsation $\Omega = 2\pi \times 10^5$. The full population is maintained in levitation for resonant frequencies despite the path multiplicity, and the central fringe sharpens over the successive cycles.

For the duration $T := T^0$, and for a sufficiently coherent atomic sample, the atomic motion in momentum -represented in Fig. 4- is periodic and bounded between two well-defined values associated with the photon recoil. The momentum confinement is provided by destructive interferences which shut off the quantum channels going out of the bounded momentum region. This remarkable property suggests an analogy with an atomic Fabry-Perot resonator in momentum space. In accordance with energy conservation, the wave-packet motion in Fig. 4 corresponds to horizontal dashed arrows. We have computed the lower-state wave-function after N resonant pulse sequences of duration $2T_0$, considering only the vertical axis without loss of generality. Each wave-packet ends up at rest, and with a momentum dispersion Δp_f . Applying the phase relation (1) succes-

sively and using a partition function approach to sum on the different paths, one obtains $\psi_a(p, t_0 + 2NT_0) = C_N e^{i\phi(\mathbf{p}, N)} e^{-\frac{p^2}{\Delta p^2}} \cos^{2N}(p/p_m)$. We have introduced the momentum $p_m = 2m/kT_0$, a global phase $\phi(\mathbf{p}, N)$ and a constant C_N . As $N \rightarrow +\infty$, multiple wave interferences thus yield an exponential momentum localization, scaled by the momentum p_m , around the rest value $p = 0$. The diffusion in altitude observed in the network of paths of Fig. 2 reflects a back-action of this localization.

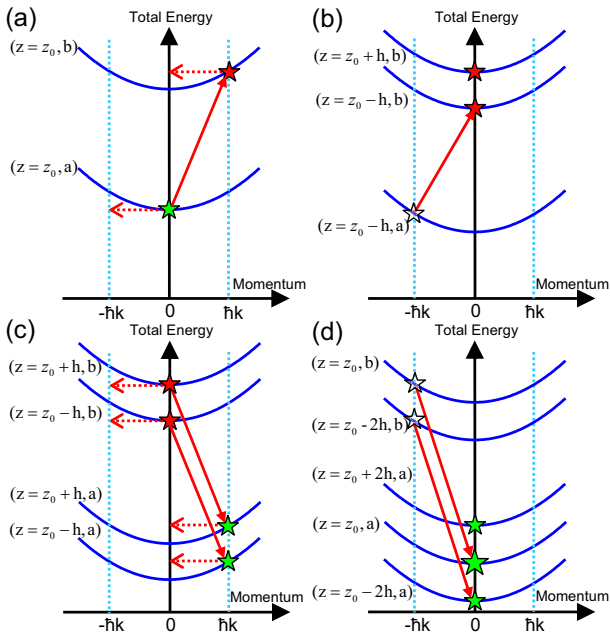


FIG. 4: Motion of the atomic wave-packets in the energy-momentum picture for the interferometer duration $2T^0$. Total energy accounts for the rest mass, the kinetic and the gravitational potential energies. Figs. (a,b,c,d), associated with the 1st, 2nd, 3rd and 4th light pulses respectively, show the packets present in coherent superposition (full stars) immediately after - or transferred (transparent stars) during - the considered pulse, whose effect is represented by a full red arrow. The atomic motion in momentum is bounded between two values associated with the photon recoil.

To summarize, we have proposed a space-time atomic sensor achieving the levitation of an atomic sample through multiple wave interference effects in a series of vertical $\pi/2$ -light pulses. The sensitivity of the levitation to a double resonance condition is used to realize a frequency or an acceleration measurement, with a sensitivity improving with the number of interfering wave-packets. At resonance, constructive multiple-wave interferences maintain the full atomic population in levitation despite the great number of non-levitating paths. The sample needs to be cooled at a subrecoil temperature in order to yield the desired interference effects. For a sufficiently dilute cloud, transverse confinement may be provided by the wave-front of spherical light pulses. This system involves no off-resonant trapping light field, so that frequency light shifts are expected to be small. In the proposed configuration the two pulse pairs are performed successively, which maximizes the interferometric area for a fixed interferometer duration; one could nonetheless also let a finite time between them. The phase-matching condition (1) can be interpreted as the equality of generalized atom-optical path in 5D [22]. This proposal has already inspired an atomic gravimeter using multiple wave interferences in levitation [23], and opens exciting perspectives for the development of optical clocks.

The authors thank S. Bize, P. Bouyer, A. Clairon, Y. LeCoq, P. Lemonde, F. Ferreira, P. Wolf for stimulating discussions, and A. Landragin, S. Walborn for manuscript reading and suggestions. This work is supported by CNRS and DGA (Contract No 0860003).

[1] S. Blatt et al., New Limits on Coupling of Fundamental Constants to Gravity Using ^{87}Sr Optical Lattice Clocks. *Phys. Rev. Lett.* **100**, 140801 (2008).
[2] T. Rosenband et al., Frequency Ratio of Al⁺ and Hg⁺ Single-Ion Optical Clocks; Metrology at the 17th Decimal Place. *Science* **319**, 1808 (2008).
[3] A. D. Ludlow et al., Sr Lattice Clock at 1×10^{16} Fractional Uncertainty by Remote Optical Evaluation with a Ca Clock. *Science* **319**, 1805 (2008).
[4] R. LeTargat et al., Accurate Optical Lattice Clock with ^{87}Sr Atoms. *Phys. Rev. Lett.* **97**, 130801 (2006).
[5] M. Takamoto et al., Improved frequency measurement of a one-dimensional optical lattice clock with a spin-

polarized fermionic ^{87}Sr isotope. *J. Phys. Soc. Jpn.* **75**, 104302 (2006).
[6] H. Katori, M. Takamoto, V. G. Pal'chikov, and V. D. Ovsiannikov, Ultrastable Optical Clock with Neutral Atoms in an Engineered Light Shift Trap. *Phys. Rev. Lett.* **91**, 173005 (2003).
[7] M. Weitz, T. Heupel, and T. W. Hänsch, Multiple Beam Atomic Interferometer. *Phys. Rev. Lett.* **77**, 2356 (1996).
[8] H. Hinderthür et al., Time-domain high-finesse atom interferometry. *Phys. Rev. A* **59**, 2216 (1999).
[9] T. Aoki, M. Yasuhara, and A. Morinaga, Atomic multiple-wave interferometer phase-shifted by the scalar Aharonov-Bohm effect. *Phys. Rev. A* **67**, 053602 (2003).

- [10] F. Impens, P. Bouyer, and C. J. Bordé, Matter-Wave Cavity Gravimeter. *Appl. Phys. B* **84**, 603 (2006).
- [11] K. J. Hughes, J. H. T. Burke, and C. A. Sackett, Suspension of Atoms Using Optical Pulses, and Application to Gravimetry. *Phys. Rev. Lett.* **102**, 150403 (2009).
- [12] G. Wilpers et al., Absolute frequency measurement of the neutral ^{40}Ca optical frequency standard at 657 nm based on microkelvin atoms. *Metrologia* **44**, 146 (2007).
- [13] A. Peters, K. Y. Chung, and S. Chu, Measurement of Gravitational Acceleration by Dropping Atoms. *Nature* **400**, 849 (1999).
- [14] C. J. Bordé et al., Optical Ramsey fringes with traveling waves. *Phys. Rev. A* **30**, 1836 (1984).
- [15] C. J. Bordé, Atomic interferometry with internal state labelling. *Phys. Lett. A* **140**, 10 (1989).
- [16] *Atom Interferometry*, edited by P. R. Berman (Academic Press, New York, 1997).
- [17] C. Cohen-Tannoudji, J. Dupont-Roc, and G. Grynberg, *Atom Photon Interactions: Basic Processes and Applications* (Wiley, New York, 1992).
- [18] T. Trebst, T. Binnewies, F. Riehle, and J. Helmcke, Suppression of Spurious Phase Shifts in an Optical Frequency Standard. *IEEE Trans. on Inst. and Meas.* **50**, 535 (2001).
- [19] C. J. Bordé, The Physics of Optical Frequency Standards Using Saturation Methods. in *Frequency Standards and Metrology* (Springer, Berlin, 1989).
- [20] M. Ben Dahan, E. Peik, J. Reichel, Y. Castin, and C. Salomon, Bloch Oscillations of Atoms in an Optical Potential. *Phys. Rev. Lett.* **76**, 4508 (1996).
- [21] C. J. Bordé, Atomic clocks and inertial sensors. *Metrologia* **39**, 435 (2002).
- [22] C. J. Bordé, 5D optics for atomic clocks and gravito-inertial sensors. *EPJ ST* **163**, 315 (2008).
- [23] M. Robert de Saint-Vincent et. al., A Quantum Trampoline for Ultracold Atoms. To be published.